An automated Test Set-up for the dynamic Characterization of IGBT Modules under different thermal and electrical Conditions

I. Hemp, L. Göhler, S. Bönisch, Hochschule Lausitz (FH), Fakultät für Ingenieurwissenschaften und Informatik, Germany, Email: Ionel.Hemp@hs-lausitz.de

Abstract

A fully automated test set-up is introduced, which permits the measurement of the terminal characteristics of an IGBT module (**I**nsulated **G**ate **B**ipolar **T**ransistor module) under different thermal and electrical conditions. Both the transients of the IGBT and the freewheeling diode are investigated separately. Additionally, a generic basic macro model of an IGBT module, which is already implemented in the system simulator Portunus®, has been validated.

1. Introduction

The use of power semiconductors in electrical circuitry increases continuously. Often, the complexity of the investigated circuit is extensive. Thus, it is aggravated to analyze the impact of switching power semiconductors on the system behavior. In particular, with regard to the transient behavior of the power semiconductors, it is necessary to investigate the terminal characteristics in a defined test environment [1]. For that reason, a test set-up for IGBT half bridge modules has been developed. The test circuit is a buck converter, which operates in hard switching mode. By means of this test set-up it is possible to investigate the transients of an IGBT and a freewheeling diode under the same thermal and electrical conditions separately. The unwanted disturbances on the transients have been reduced as much as possible by a low inductance design of the IGBT test set-up. To incorporate the influence of EMI in a circuit simulation it is necessary, to use more realistic models of the power semiconductors than simple switches and ideal didoes. In the used system simulator Portunus® a generic basic macro model of an IGBT module is implemented, which can be adapted and tuned with a set of parameters [4]. For this reason, an equivalent circuit of the test set-up has been built up in Portunus® to validate the macro model in one operating point. This parameterized macro model will be applied in a resonant transition switching welding power supply [2] [3] simulation to investigate the EMI behavior of the system design [4].

2. Measurement Requirements and IGBT Test Set-Up

The measurement requirements for the terminal values of an IGBT module have been defined as follows. Typically, the rise time and fall time of power semiconductors rated for medium currents (e.g. IGBTs and MOSFETs) are in the range of some ten nanoseconds. From the data sheet of the device under test (DUT) a minimum bandwidth for the voltage and current probes of 20MHz can be determined by the fall time. To avoid measuring error, it is recommended to use probes with the four times of the minimum bandwidth. In the following table the properties of the applied probes are listed. Due to the low inductance design of the coaxial shunt a high bandwidth can be achieved. This measuring method of the operating currents is suited for temporarily pulsed applications, because the dissipated power of the coaxial shunt is limited. To benefit from the high bandwidth, a low inductance connection is essential.

No.	Terminal Quantity (IGBT)	Type	Bandwidth	No.	Terminal Quantity (IGBT)	Type	Bandwidth
1	collector current	coaxial shunt	DC–1GHz	3	gate-emitter voltage	diff. probe	200MHz
2	gate current	current clamp	DC–100MHz	4	collector-emitter voltage	diff. probe	200MHz

Table 1 Measurement accessories

Fig. 1 b) illustrates the 62mm IGBT module, which contains two IGBTs and their associated freewheeling diodes. The terminals 1 to 3 are connected to the load and the main DC supply of the test set-up, whereas the terminals 4 to 7 control the IGBTs (Fig. 1 a).

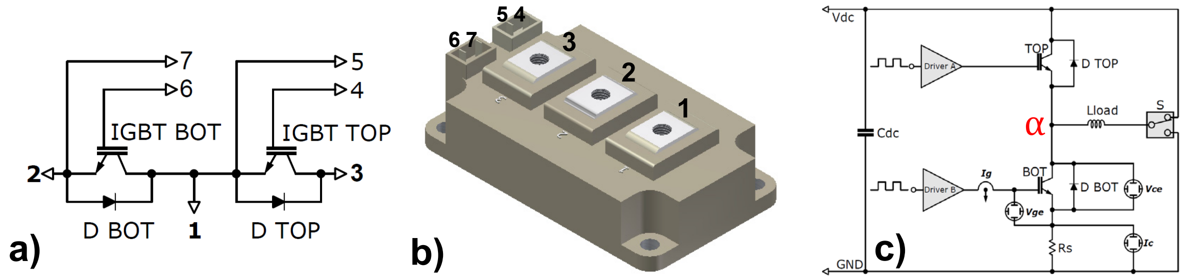

Fig. 1. **a)** Electric schematic without parasitic elements of the half bridge module **b)** 62mm IGBT half bridge module **c)** Basic circuit of the test tet-up for half bridge modules

As mentioned before, the IGBT module operates in hard switching mode. Fig. 1 c) shows the circuit scheme of the test- and the measurement set-up. By switching a contactor S the analysis mode is selected. Therefore the IGBT and the freewheeling diode can be investigated under the same electrical and thermal conditions. The advantage of this test set-up is the high reproducibility of measurements, because it is fully automated. If the contactor S is connected to the positive pole of the DC voltage supply, the BOT IGBT will be switched, whereas the TOP IGBT is still turned off. The current commutation occurs between D TOP and BOT IGBT. As soon as the contactor is switched to the ground terminal GND, the TOP IGBT will be operated, whereas the BOT IGBT remains off. In this case the load current commutates between TOP IGBT and the freewheeling diode D BOT.

3. Characterization Methodology

A commonly used method for the characterization of power semiconductors is the double-pulse experiment. Two independent and freely configurable gate pulses turn on the IGBT for a predetermined time. How fast an IGBT turns on and off basically depends on the gate resistances, the voltage level of the driver, and the characteristics of the IGBT itself.

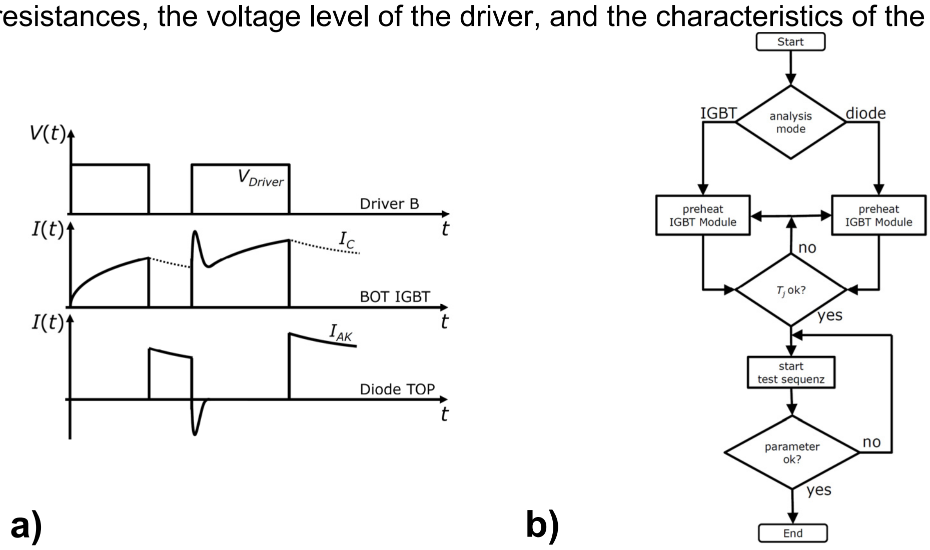

Fig. 2. **a)** Transients of the BOT IGBT, freewheeling diode, and the driver voltage without influence of parasitic effects with respect to simplified commutation conditions **b)** Flow chart of the characterization methodology

Fig. 2 a) depicts the transients of an IGBT module qualitatively, if the contactor *S* is switched to the positive DC voltage supply. A simplified flow chart of the double-pulse experiment is shown in Fig. 2 b). At the first step the analysis mode can be chosen. Afterwards the desired junction temperature is adjusted by heating the DUT. Once the set temperature has been reached, the double-pulse experiment is ready to start. If the predetermined test conditions have been achieved, the test sequence is completed. If deviations in the test conditions exist, the parameters need to be adjusted.

4. Measurement Results

This chapter deals with the measurement results of the double pulse experiment under certain thermal and electrical conditions. In the first experiment the junction temperature T_j has been varied from 80°C – 125°C for otherwise identic electric conditions. A further experiment shows the results at a constant junction temperature T_j = 125°C but under different gate driver design conditions. Table 2 summarizes the experiment parameter variation. During the measurements the TOP IGBT (Fig. 1 c) is always turned off. The current commutation occurs between the freewheeling diode D TOP and the BOT IGBT.

No.	IGBT FF300R12KS4				
	Parameter	Symbol	Unit	Value A	Value B
1	DC link voltage	V_{DC}	V	600.0	600.0
2	Collector current slope	dI_C/dt	A/µs	40.0	40.0
3	Maximum collector current	$I_{C,max.}$	A	90.0	90.0
4	Gate turn on resistor	$R_{g,on}$	Ω	4.7	2 x 4.7
5	Gate turn off resistor	$R_{g,off}$	Ω	2.45	2 x 2.45
6	Junction temperature	T_j	°C	80/125	125

Table 2 Test conditions for the double-pulse experiment

4.1. Temperature Influence of the Transient Behavior

In this experiment the junction temperature has been increased from 80°C – 125°C (Table 3 A). At a higher junction temperature a lower carrier mobility and an increased carrier lifetime can be expected. At the first turn-on pulse (Fig. 2 a) of the BOT IGBT the potential change at terminal α (Fig. 1 c) occurs a collector current peak. This dielectric current is caused by the junction capacitances of the TOP IGBT and the TOP Diode. The measured collector-emitter voltage V_{ce} and the collector current I_c (Fig. 3 a) do not differ substantially, because the collector current slope is limited to 40A/µs by a low resistance air-coil load (15µH). This current slope restricts the impact of the forward recovery behavior during the first turn-on pulse. Fig. 3 b) depicts the first turn-off pulse. At 2.6µs the gate driver outputs the negative voltage level (-12V) and the IGBT input capacitance C_{ies} is discharged by the (negative) gate current I_g. Since I_g reduces the channel current of the inherent MOSFET the carrier densities start to decrease. How fast V_{ce} rises depends on the gate-collector capacitance C_{gc}, the carrier extraction and recombination and the gate current level I_g. At 3.1µs a time delay of 18ns occurs, caused by the higher carrier mobility at lower temperature and the increased carrier lifetime at higher temperature primarily, because the temperature-influence of C_{gc} at reverse bias voltages is negligible. The junction temperature influence on the current slope dI_c/dt and the voltage slope dV_{ce}/dt at T_j = 80°C and Tj = 125°C is not significant. The main limiting factors for the current slope at turn-off are the sum of the stray inductances inside the commutation cell, the forward recovery behavior of the diode and the qualities of the IGBT itself. When V_{ce} attains DC voltage supply (600V) oscillations occur which are caused by the effective stray inductance of the test set-up, IGBT module and the output capacitance C_{oes} of the IGBT module (BOT IGBT and D TOP). Fig. 2 c) shows the second turn-on pulse. Once V_{ge} reaches the threshold voltage V_{th} the collector current I_c begins to flow. The reduction of V_{ce} at 6.25µs results from the total stray inductance (for very fast IGBT). Due to the stray inductance of the auxiliary-emitter (some nH) inside the main current path of I_c the transient voltage increases the gate-emitter voltage V_{ge} temporarily. The crucial difference between various junction temperatures is the higher reverse recovery current peak and the extended tail current-phase of the diode. The main reason is the risen carrier density inside the semiconductor layers due to the elevated carrier lifetime.

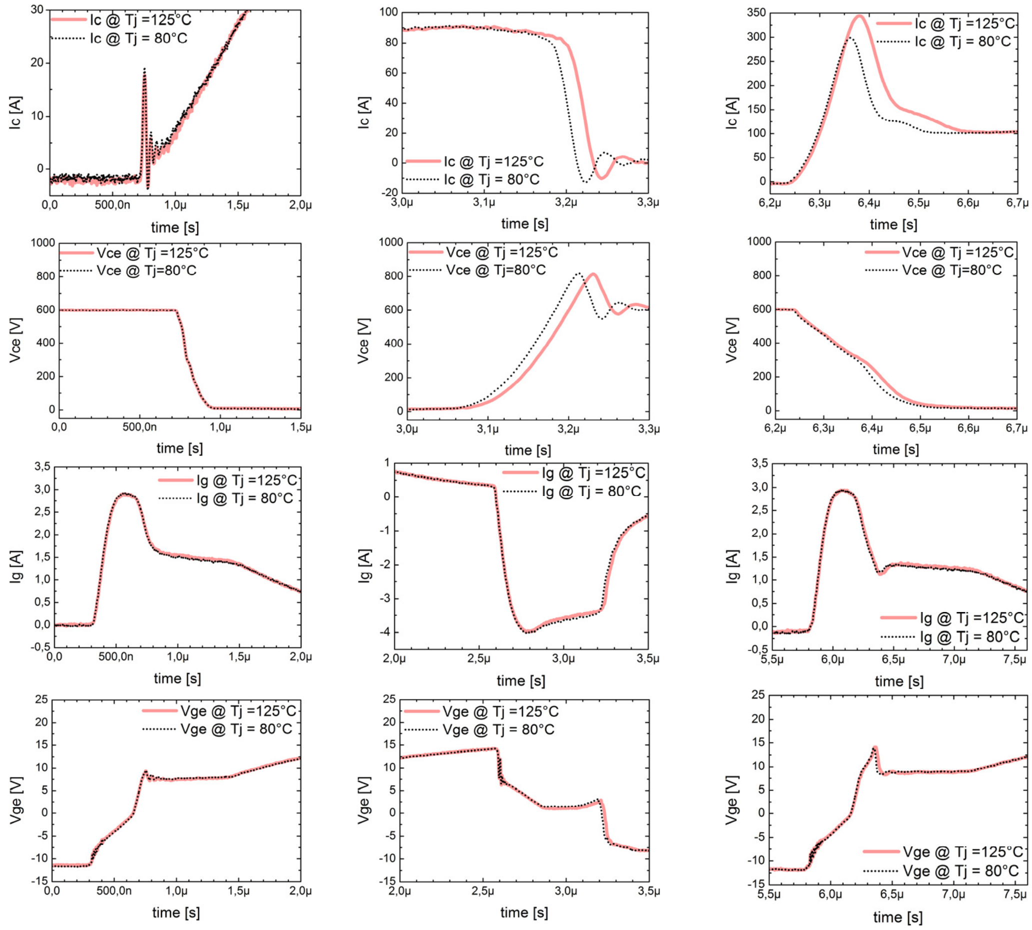

a) b) c)

Fig. 3. Terminal characteristics of the IGBT module FF300R12KS4 **a)** first turn-on pulse **b)** first turn-off pulse **c)** reverse recovery current during the second turn-on pulse

4.2. Gate-Resistor Influence of the Transient Behavior

To investigate the influence of the current slope dI_c/dt and the voltage slope dV_{ce}/dt the turn-on and turn-off gate resistors ($R_{g,on}$, $R_{g,off}$) have been varied (Table 2 B). By doubling the value of $R_{g,on}$ a lower gate current I_g charges the gate-collector capacitance C_{gc} and the gate-emitter capacitance C_{ge} slower. This leads to the extended plateau of V_{ge}. The voltage slope dV_{ce}/dt is reduced by 40% (Fig. 4 a) hence the current peak of I_c is lower. As well as $R_{g,on}$, the resistance of $R_{g,off}$ has been doubled too (Table 2 B). At the turn-off pulse (Fig. 4 b) the lower gate current discharges C_{gc} and C_{ge} slower and leads to extended plateau of V_{ge} similarly to turn-on. The voltage slope dV_{ce}/dt during turn-off is 20% lower whereas the current slope dI_c/dt remains widely similar, because the turn-off current slope is not controllable by the gate turn-off resistor. Since I_c can be also controlled by the gate resistor, dI_c/dt is reduced by more than 30% (Fig. 4 c). However, it is recommended to control dI_c/dt and dV_{ce}/dt by using an advanced driver circuit design [6] because the dissipated power at turn-off is considerable. In addition, the reverse recovery peak current I_{rr} is reduced by 21% because the carrier extraction of the diode is more moderate and the stored charge is more reduced by carrier recombination.

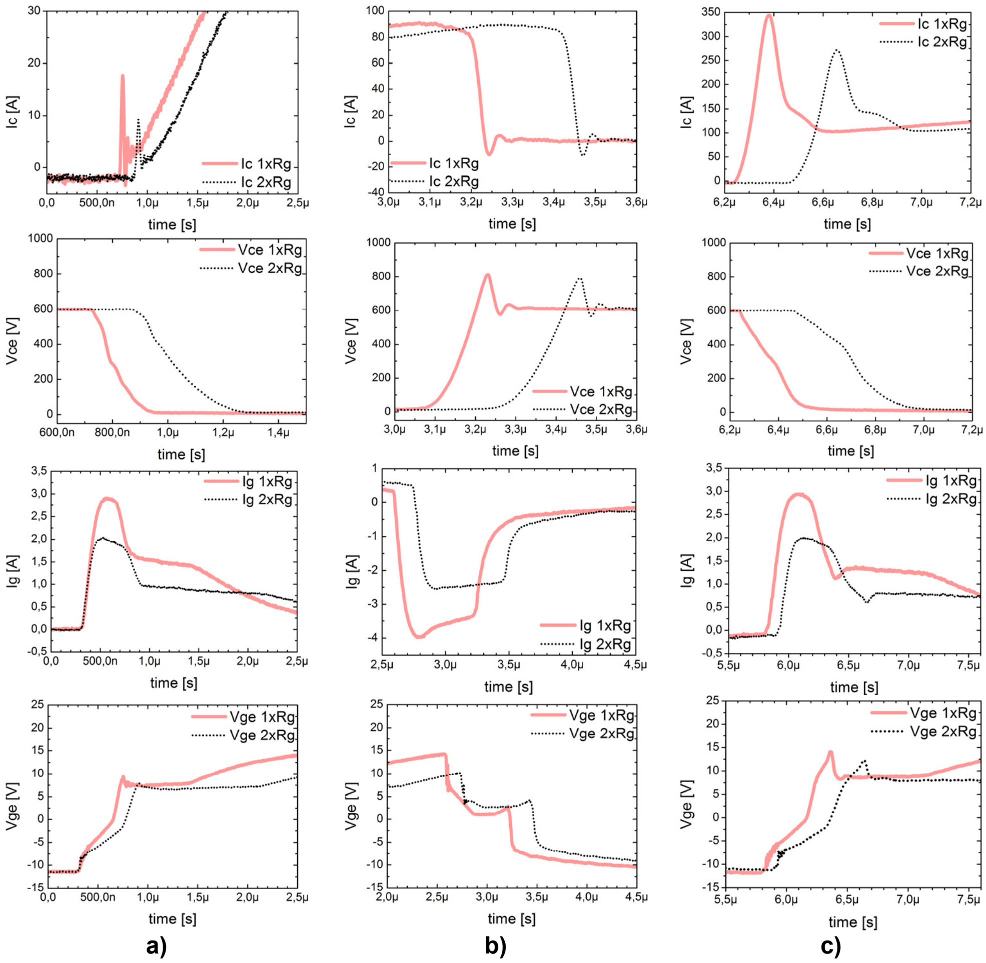

Fig. 4. Terminal characteristics of the IGBT module FF300R12KS4 **a)** first turn-on pulse **b)** first turn-off pulse **c)** reverse recovery current during the second turn-on pulse

5. Active Component Modeling

For the IGBT modules, an adapted macro model is used [4]. This macro model can be tuned with a set of parameters, which can be derived from the data sheet of the manufacturer and simple measurements.

5.1. IGBT Macro Model

Power semiconductors such as IGBTs and diodes are the main noise source in switched power supplies. In the investigated high power current source two half bridge modules are used. Therefore a sufficiently accurate model for IGBT modules is needed to predict the terminal characteristics. The simulation software Portunus® provides an adapted macro model of an IGBT module. Its parameter set can be extracted from the data sheet. The IGBT model consists of two parts. The first part includes the static transfer and output characteristic. The second part models the transient behavior, which strongly depends on the voltage-dependent semiconductor capacitances and the carrier mobility and lifetimes as well as the parasitic elements of the IGBT module.

In Fig. 5 the adapted macro model of an IGBT and the associated freewheeling diode is shown. The static characteristics of the IGBT are modeled by a voltage controlled current source (I_{transf}) and a diode (D_{out}). Since the IGBT operates as a switch, the description of the transfer and output characteristics in the saturation region is required. They are implemented as look up tables. All static losses have been assigned to the diode D_{out}. If the gate-emitter voltage V_{ge} reaches the threshold voltage V_{th}, the collector current I_C begins to flow through the source I_{transf} and the diode D_{out}. The diode D_{ideal}, is an ideal device, which conducts a current equal to the difference between $I_{transf} = f(V_{ge})$ and the collector current. Theoretically, all capacitances between the terminals of the IGBT are voltage dependent and affect the dynamic behavior. However, the capacitance change of C_{ge} due to a variation of V_{ge} is relatively small, so that C_{ge} is assumed constant. The capacitance of C_{gc} varies by a factor of more than ten under typical operation conditions. This behavior is modeled by equation (1).

$$C_{gc} = C_0 \cdot \left(1 - \frac{V_{gc}}{V_{diff}}\right)^{-0.5} \quad (1) \qquad I_{ABM1} = K_{tail} \cdot \sqrt[3]{I_{tail0}^2} \cdot \left(1 - \sqrt{\frac{V_{ce}}{V_{ces}}}\right)^{-1} \quad (2) \qquad C_d = \frac{\tau_0}{V_T} \cdot I_S \cdot \left(\exp\left(\frac{V_{ak}}{V_T}\right) - 1\right) = \tau_0 \cdot \frac{I_d}{V_T} \quad (3)$$

If the Gate-Collector voltage V_{gc} reaches the diffusion voltage V_{diff} in the model equation, the capacitance of equation (1) is limited to an upper bound. With the help of the voltage source V_{shift} the operating point of the capacitance curve is shifted. The high frequency characteristic curve of C_{gc} and C_{ce} can be extracted from the datasheet. Since the ratio of the collector-emitter capacitance C_{ce} of the IGBT and the junction capacitance of the freewheeling diode are unknown, the effect is modeled by one junction capacitance C_{spr}. To reduce the amplitude of oscillations, an auxiliary resistor R_{cj} is used. The slope of the gate-emitter voltage V_{ge} depends on the internal gate resistance $R_{g,int}$, the output characteristics of the gate driver circuit, the input capacitance C_{ies} of the IGBT and the stray inductances in the gate circuitry. $R_{g,int}$ is the sum of the poly silicon (gate material) resistance, bond wires resistances and the contact resistances. The tail current of the IGBT is modeled by an auxiliary network (Fig. 5). If the current flows through the diode D_{out}, the measured current I_{tail0} is fed into to the current source ABM1. Equation (2) is a combination of experimental investigations and fundamental semiconductor equations. This expression is used in ABM1.

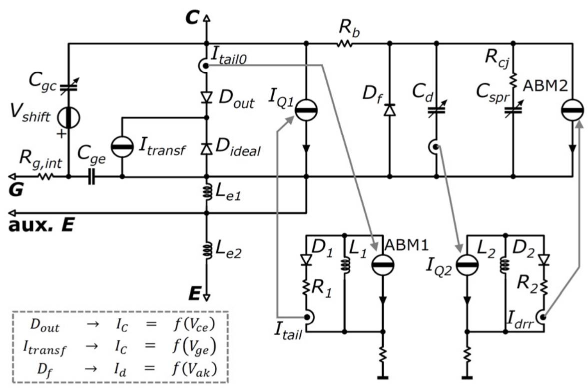

Fig. 5. Generic macro model of the IGBT moulde

As long as there is a current ABM1 flowing through the source ABM1, energy is still stored in the inductance L_1 and the ideal diode D_1 blocks. When the current through ABM1 vanishes, L_1 acts as a source, and the current flows through resistor R_1. The current decay is hence defined by L_1 and R_1. The measured current I_{tail} is fed into the current source I_{Q1}, which emulates the tail current of the IGBT. The reverse recovery current I_{drr} of the freewheeling diode is modeled similarly. The measured current of I_{Q2} is caused by the diffusion capacitance C_d (Eq. 3). This equation is valid for a low power *pn*- diode (i.e. low-level injection) with an abrupt *pn*-junction only. All model parameters (except τ_0) can be extracted from the DC characteristic of the freewheeling diode, and τ_0 is estimated using the reverse recovery charge. R_b is the effective ohmic resistance of the freewheeling diode. Table 3 resumes the model parameters for the IGBT and the freewheeling diode.

No.	IGBT					Freewheeling Diode			
	Parameter	Sym.	Unit	Value		Parameter	Sym.	Unit	Value
1	Blocking voltage	V_{ces}	V	1200.0	15	Series resistance	R_b	Ω	$5.6 \cdot 10^{-3}$
2	Reverse Saturation current	I_{ces}	A	$1{,}0 \cdot 10^{-3}$	16	Voltage drop in an opertation point	V_{f1}	V	1.0
3	Int. gate resistance	$R_{g,int}$	Ω	1.0	17	Diode current in an operating point	I_{f1}	A	64.0
4	Minimum input capacitance	$C_{ies,min}$	F	$58 \cdot 10^{-9}$	18	Satuaration current	I_S	A	$0.5 \cdot 10^{-3}$
5	Maximum input capacitance	$C_{ies,max}$	F	$133 \cdot 10^{-9}$	19	Diffiusion voltage	V_{exp}	V	0.614
6	Minimum Gate-collector capacitance	$C_{gc,min}$	F	$3.5 \cdot 10^{-9}$	20	Thermal voltage	V_T	V	0.546
7	Gate-emitter capacitance	C_{ge}	F	$54.5 \cdot 10^{-9}$	21	Blocking resistance	R_{spr}	Ω	$2.4 \cdot 10^{6}$
8	Gate-collector capacitance @ 0V	C_{02}	F	$78.5 \cdot 10^{-9}$	22	Minority carrier life time 1	t_{rr}	s	$218.4 \cdot 10^{-9}$
9	Diffiusion voltage	V_{d02}	V	$69.7 \cdot 10^{-3}$	23	Minority carrier life time 2	t_{rrt}	s	$75.0 \cdot 10^{-9}$
10	Shift voltage for C_{gc}	V_{cgc}	V	6.0	24	Junction capacitance @ 0V	C_{01}	F	$16.8 \cdot 10^{-9}$
11	Collector-emitter inductance	L_{ce}	H	$15 \cdot 10^{-9}$	25	Auxiliary resistor	R_{Cj}	Ω	20.0
12	Stray inductance of aux. emitter	L_{he}	H	$1.5 \cdot 10^{-9}$					
13	Time constant for tail current	tau_{Hl}	s	$1.0 \cdot 10^{-12}$					
14	Factor for model equation (2)	K_i	–	$1.0 \cdot 10^{-12}$					

Table 3 IGBT macro model parameter @ T_j = 125°C

5.2. Test Conditions and Simulation Results

A simple test circuit for half bridge modules has been built up in Portunus® to verify the terminal characteristics of the IGBT module at the desired operating point. For comparison, a chopper with double-pulse gate control is used. Two independently and freely configurable gate pulses turn on the BOT IGBT (Fig. 1 c) for a predetermined time under defined test conditions. Table 2 Value A (T_j = 125°C) summarizes the test conditions. To ensure a constant collector current slope of 40A/µs, a low-resistance air-coil load of 15µH has been used. Since the influence of self-heating must be low, short test pulses (3µs) are generated. Fig. 6 illustrates the results from the measurement and compares them to the simulation. As the fitted IGBT macro model is used for EMI simulation [3] it is reasonable to focus on good agreement between simulated and measured output characteristics. This concerns the collector current I_c and the collector-emitter voltage V_{ce}. The definition of a relative model error with respect to the typical switching times is partly possible, because I_C and V_{ge} do not reach steady state. Therefore, the model error for turn-on delay $T_{D,on}$, turn- on time T_{on}, turn off delay $T_{D,off}$, and turn off time T_{off} cannot be specified meaningfully.

A good match of the voltage slope (dV_{ce}/dt) between measurement and simulation for turn-off has been achieved. The relative error is less than 18% whereby the error for fall time T_f is about 11%. At 300ns the simulated gate-emitter voltage V_{ge} differs from the measurement, because the modeled gate-emitter capacitance C_{ge} is assumed to be constant (Fig. 6 a). Since the collector current I_c flows for the first time (700ns) the simulated current peak is reduced, and the plateau of V_{ge} lasts longer. This is caused by the lower voltage slope dV_{ce}/dt and capacitance model of C_{gc}. The relative error can be reduced by fine-tuning the model parameters. Additionally, the simulated and measured transients of I_C and V_{ce} for turn-off (Fig. 6 b) show a good agreement in amplitude and slope. The reverse recovery current peak I_{rr} is equal to the measured value (Fig. 6 c). However, the current slope error at 6.25µs is significant. The relative model error for rise time T_r is 35%. The main reasons are the value of the total stray inductance, the higher small-signal transconductance g_f of the IGBT, compared to the transfer characteristic in the datasheet, and the temporarily increase of the gate-emitter voltage V_{ge} influenced by the models of the gate-collector and the gate-emitter capacitance (C_{gc}, C_{ge}). The voltage error of V_{ce} during reverse recovery results from the decreased current slope (Fig. 6 c), thus the transient inductive voltage drop is lower.

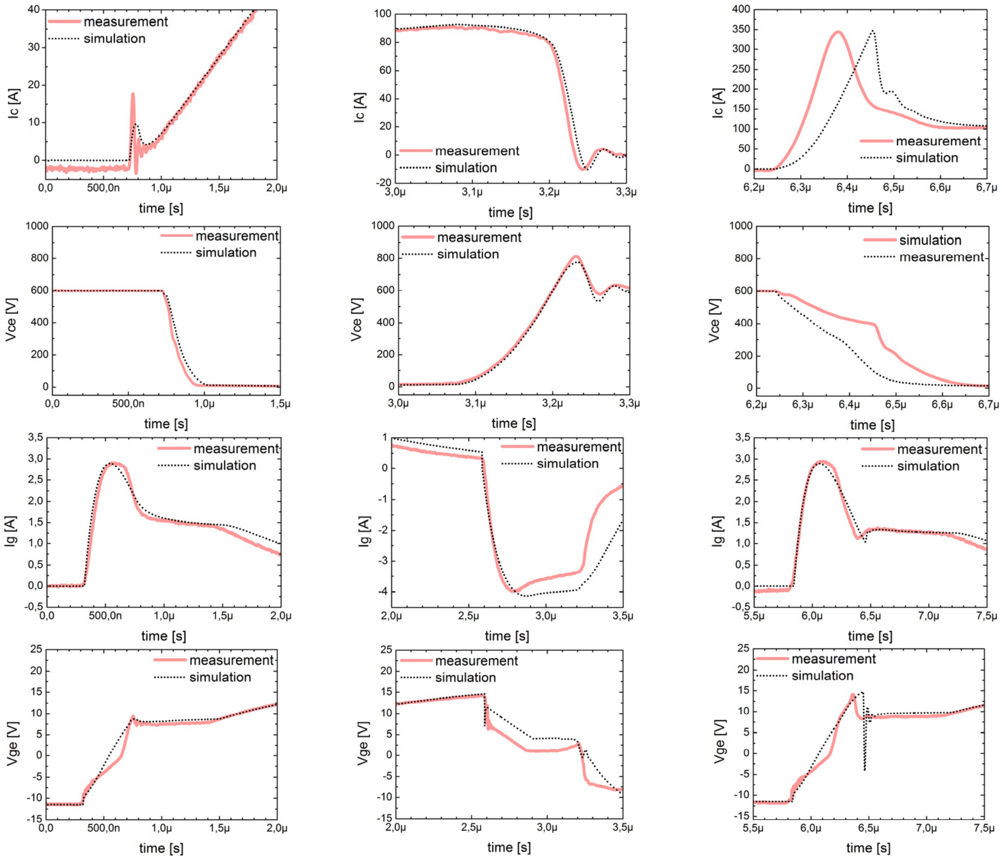

a) b) c)

Fig. 6. Terminal characteristics of the IGBT module FF300R12KS4 **a)** first turn-on pulse **b)** first turn-off pulse **c)** reverse recovery current during the second turn-on pulse

6. Conclusion

It has been shown how powerful the temperature influence of T_j is. The impact on the reverse recovery current of the diode is mainly given by the increased carrier lifetime. Furthermore, the influence on the transient behavior of V_{ce} and I_c during turn-off is negligible. Using higher gate turn-on and turn-off resistors, the impacts on the reverse recovery current as well as current and voltage slopes (dV_{ce}/dt, dI_c/dt) are significant. During the second turn-on state a voltage slope reduction of 20% and current slope reduction of 30% has been achieved. However, it is recommended to control dI_c/dt and dV_{ce}/dt by using an advanced driver circuit design, because the dissipated power at turn-off is considerable. Additionally, a chopper with double-pulse gate control has been built up to validate the terminal characteristics of the IGBT macro model.

7. Literature

[1] M. Helsper, F. W. Fuchs, R. Jakob, “Measurement of dynamic characteristics of 1200A/1700V IGBT-modules under worst case conditions, “Nordic Workshop on Power and Industrial Electronics”, NORPIE 2000, Aalborg, 2000

[2] Oliver D. Patterson and Deepakraj M Divan, “Pseudo-Resonant Full Bridge DC/DC Converter” IEEE Transactions On Power Electronics, vol. 6, no. 4, October 1991, pp. 671–678

[3] N. Fröhleke, H. Mundinger, S. Beineke, P. Wallmeier, H. Grotstollen, “Resonant Transition Switching Welding Power Supply“, IEEE Industrial Electronics Society International Conference (IECON97), New Orleans, 1997, pp. 615–620

[4] D. Bucke, I. Hemp, L. Göhler, S. Bönisch, EMC Europe “Conducted emission simulation of an industrial high power current source”, EMC Europe, Brugge, 2013

[5] A. Wintrich, “Verhaltensmodellierung von Leistungshalbleitern für den rechnergestützten Entwurf leistungselektronischer Schaltungen“, Promotion, Technische Universität Chemnitz, 1996

[6] C. Gerster, P. Hofer, “Gate-controlled dv/dt- and di/kdt limitation in High Power IGBT Converters”, EPE Journal, Vol 5 no 3/4, Jan. 1996, pp. 11—16